

## RESEARCH ARTICLE



# Examining the Use of the Watershed Algorithm for Segmenting Crown Closure on a Dry Land Forest

Dwika Hardian Afriansyah<sup>a</sup>, I Nengah Surati Jaya<sup>b</sup> and Muhammad Buce Saleh<sup>b</sup>

## Article Info:

Received 29 August 2022

Revised 19 February 2024

Accepted 15 April 2024

<sup>a</sup>Departement of Forest Management, Faculty of Forestry and Enviroment, IPB University, Bogor, indonesia, 16680

## Corresponding Author:

Dwika Hardian Afriansyah  
Department of Forest  
Management, Faculty of Forestry  
And Enviroment, IPB  
University, Bogor, Indonesia  
E-mail: [ins-jaya@apps.ipb.ac.id](mailto:ins-jaya@apps.ipb.ac.id)

Copyright © 2024 Alfriansyah et al. This is an open-access article distributed under the terms of the Creative Commons Attribution (CC BY) license, allowing unrestricted use, distribution, and reproduction in any medium, provided proper credit is given to the original authors.



## Abstract

This study used a watershed algorithm to detect canopy cover in dryland forests. The objective of this study was to determine the best parameters of the watershed segmentation algorithm to obtain information on crown closure from filtered and unfiltered high- and very-high-resolution images. The best performance of each parameter combination of the tolerance value (T), mean value (M), and variance value (V), which is written as C:[T]-[M]-[V], is determined based on the level of accuracy. This study used Pleiades-1B and SPOT-6 images as primary digital data. The results showed that the low-pass filtered Pleiades-1B image showed the best performance with a combination of parameters C6-MF:[10]-[0.7]-[0.3], with an overall accuracy (OA) of 91.0% and an accuracy Kappa (KA) of 83.2%. The low-pass filtered Spot-6 image shows a combination of parameters C7-MF:[10]-[0.8]-[0.2], which has an accuracy of 90.6% OA and 65.4% KA. This study concludes that the filtered image with a low-pass filter always yields more accurate results than the original data (without a filter) for both Pleiades-1B and SPOT-6 images. The very high spatial resolution provides better accuracy than the high spatial resolution.

Keywords: *Low-pass filter, Pleiades-1B, Spot-6, Superpixel, Watershed Algorithm*

## 1. Introduction

Satellite imagery with high and very high spatial resolution has presented enormous opportunities and challenges for forest inventories, where image classification can no longer rely on a pixel-based approach. The object-based approach is more effective when the image has a high spatial resolution, with a pixel size of less than 1.5 m. The watershed algorithm is one of the simplest algorithms that has not been widely used for canopy-closure segmentation. This algorithm provides an excellent perspective to detect canopy cover semi-automatically, which is one of the key variables in estimating stand volume and forest carbon stock. Mathematical models for estimating stand stocks often use variable canopy cover as the most applicable variable for forest inventories. The crown closure variable is the most practical visual interpretation variable commonly used in predicting either the timber technique or biomass stock using high and very high spatial resolutions. In practice, estimating stand volume using the variables of crown closure (canopy cover), number of trees, and tree crown diameter may result in an average error of < 10%. However, this level of accuracy can generally be achieved only by experienced foresters with skillful knowledge of image analysis. Crown closure can be obtained quickly, accurately, and consistently using high- and high-resolution imagery. Object-based methods for dealing with objects consider the color, size [1], shape, and texture of the analyzed object [2]. Therefore, it is necessary to examine a more quantitative approach that applies automatic or semiautomated methods to obtain crown closures. The quantitative approach tested here combines both pixel- and object-based algorithms.

The watershed algorithm considers the mean and variance of the bands that are used to determine the segmentation of each class. The watershed algorithm shows perfect accuracy in hyperspectral images[3]. In addition, a segmentation method using the watershed algorithm shows that this method is very effective for image segmentation[4]. Using the watershed algorithm for boreal forest classification has also shown excellent results[5]. There is still no research on watershed algorithms, especially for canopy and slit classification; therefore, there is a need for research using watershed algorithms for canopy closure

segmentation. Watershed algorithms classify land use and cover [6], settlement extraction [7], and satellite-based rainfall forecasts [8]. Studies on very high spatial resolution image segmentation for tropical forest classification using watershed algorithms have not yet been conducted. The objective of this research was to find the best segmentation parameters using the watershed algorithm for classifying tree canopies in tropical forests using Pleiades-1b images, both with and without filters.

## 2. Research Methodology

### 2.1 Research Area

The study site was located in a concession area in the Bulungan Regency, North Kalimantan Province. Geographically, the study site is situated between  $20^{\circ}09'199''$ – $30^{\circ}34'48''$  S and  $116^{\circ}04'41''$ – $117^{\circ}57'56''$  East Longitude (Figure 1). Data were collected from December 23 to 28, 2020. The data were analyzed at the Remote Sensing and GIS Laboratory, Department of Forest Management, Faculty of Forestry, IPB University.

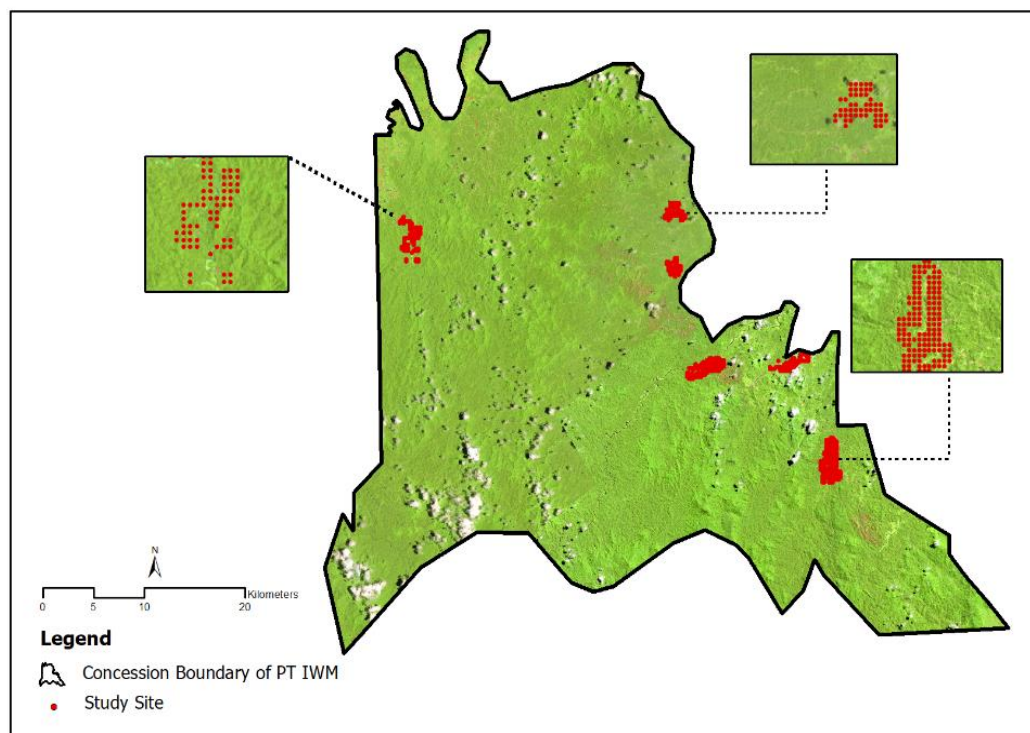


**Figure 1.** Sampling sites in the anchialine habitat of red shrimp at Koguna Beach area, Buton Island

### 2.2 Material

Segmentation in research using software TerrSet Geospatial and Modeling 18.31. This study uses ArcMap 10.3 for spatial analysis, while ERDAS Imagine was used for image filtering. In addition, the research is equipped with measuring tape, phi-band, clinometer, compass, GPS, camera, tally sheet, and other stations for land data collection. The image data were high-resolution images (Pleiades-1B Image) and high-resolution images (Spot-6).

**Table 1.** Data characteristics (Pleiades 1B image)

Band	Wavelength	Spatial Resolution
Band 1 (Blue)	430 nm	2 m
Band 2 (Green)	490 nm	2 m
Band 3 (Red)	600 nm	2 m
Near Infrared	750 nm	2 m
Pancromatic	480 nm	0.5 m

**Table 2.** Data characteristics (Spot 5-6 image)

Band	Wavelength	Spatial resolution
Band 1 (Blue)	485 nm	6 m
Band 2 (Green)	560 nm	6 m
Band 3 (Red)	660 nm	6 m
Near-infrared	825 nm	6 m
Panchromatic	597,5 nm	1.5 m

**2.3 Method**

A sample plot was developed by considering the representativeness of the forest conditions and road networks for accessibility. The plot size was 50 m × 50 m. Thirty samples were taken for each image, either on the Pleiades 1 B image or the spot-6 image. Trees were measured in all quadrants I-IV, but the poles were measured only in a 10 m × 10 m subplot of quadrants II and IV (see Figure 2). Image preprocessing involves data format conversion, geometric correction, image mosaic, and image cropping. In this study, the original image format was Geotiff and was then converted into the Terrset ASCII format. Before the mosaicking process, the study carried out histogram equalization. This study also crops the area of interest to be fully processed in this study.

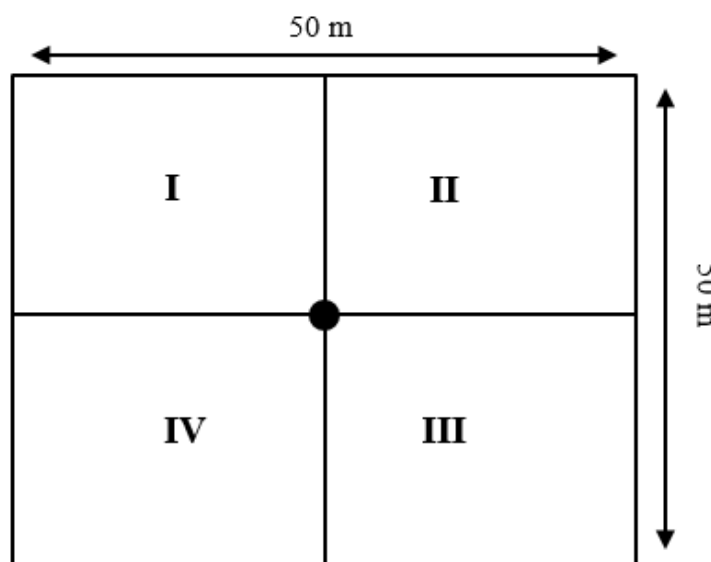


**Figure 2.** Research sample plot design

Filtering satellite images is necessary to remove unwanted interference. This activity aims to smoothen the image by removing unnecessary small blotches caused by canopy shadows and small gaps in the tree branches or twigs. Some researchers used median and mean filters[9]. Mean filtering is part of the low-pass filter used for image refinement and aims to reduce the spatial frequency of the data. weakness of watershed segmentation is its sensitivity to noise disturbances. Higher pixel

variations often cause excessive segmentation; therefore, filtering and smoothing techniques [10] are required to minimize this interference with a  $3 \times 3$  width to smooth the images [11]. The parameter values used in this study are listed in (Table 3).

Segmentation divides a digital image into several regions to be analyzed and used to distinguish different objects in an image. Watershed algorithm is a segmentation technique that combines edge and region-based information [12]. Watershed segmentation relies on the principle that a grayscale image can be viewed as a topographic surface, where the digital value for each pixel can be considered the elevation at that point [13]. The parameters used in the watershed algorithm were the window width, mean weight factor, similarity tolerance, and weight variance factor.

**Table 3.** Combination of watershed algorithm segmentation parameters on very high-resolution satellite imagery (Pleiades-1b image) and high-resolution satellite imagery (SPOT-6)

No	Combination Code	Similarity Tolerance	Mean Factor	Variance Factor	Combination
1	C1	10	0.2	0.8	[10]-[0.2]-[0.8]
2	C2	10	0.3	0.7	[10]-[0.3]-[0.7]
3	C3	10	0.4	0.6	[10]-[0.4]-[0.6]
4	C4	10	0.5	0.5	[10]-[0.5]-[0.5]
5	C5	10	0.6	0.4	[10]-[0.6]-[0.4]
6	C6	10	0.7	0.3	[10]-[0.7]-[0.3]
7	C7	10	0.8	0.2	[10]-[0.8]-[0.2]
8	C8	20	0.2	0.8	[20]-[0.2]-[0.8]
9	C9	20	0.3	0.7	[20]-[0.3]-[0.7]
10	C10	20	0.4	0.6	[20]-[0.4]-[0.6]
11	C11	20	0.5	0.5	[20]-[0.5]-[0.5]
12	C12	20	0.6	0.4	[20]-[0.6]-[0.4]
13	C13	20	0.7	0.3	[20]-[0.7]-[0.3]
14	C14	20	0.8	0.2	[20]-[0.8]-[0.2]
15	C15	30	0.2	0.8	[30]-[0.5]-[0.5]
16	C16	30	0.3	0.7	[30]-[0.4]-[0.6]
17	C17	30	0.4	0.6	[30]-[0.3]-[0.7]
18	C18	30	0.5	0.5	[30]-[0.2]-[0.8]
19	C19	30	0.6	0.4	[30]-[0.6]-[0.4]
20	C20	30	0.7	0.3	[30]-[0.7]-[0.3]
21	C21	30	0.8	0.2	[30]-[0.8]-[0.2]

A Super pixel is a collection of pixels, based on their intensity values [14]. The use of primarily Cluster-based super pixels has been widely used in previous research studies, such as those by Tang et al. [15], for labeling [16] and detection [17]. In this study, labeling was performed on superpixels or regions resulting from segmentation. This is more effective than labeling pixels [18] because the superpixel can carry more information from the segmentation results than the information from the pixels. In addition, super pixels can maintain object boundaries well; labeling the segmentation results is performed using segment ID or training sample to determine the canopy and gap the values in the superpixel class, in which the training area used is based on the superpixel results from segmentation and field validation (ground truth). The pixel-based category provided superpixel clusters in highly similar segments. Training sample selection must consider the spatial resolution and availability of remote sensing data.

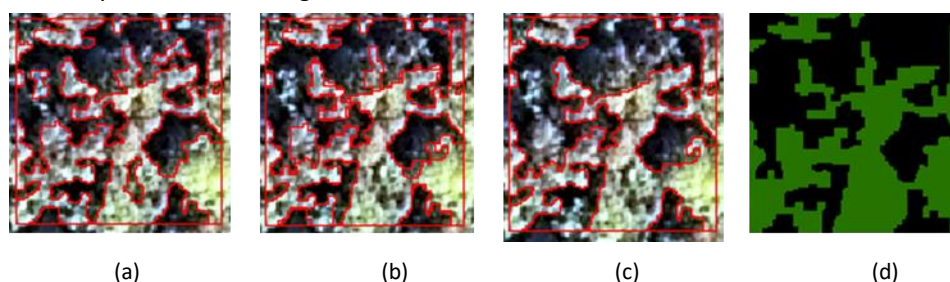


**Figure 3** (a). Object classification using the watershed algorithm (b) pixel classification (c) the object classification and pixel classification result intersect (d) segmentation classification; canopy and gap

To determine the reliability of the segmentation results, the authors tested the accuracy of several combinations of segmentation parameters in the watershed algorithm and evaluated the overall accuracy (OA) and kappa accuracy (KA). Accuracy was considered good if it had an overall accuracy value above 85%.

$$\text{Overall Accuracy (OA)} = \frac{\sum_{i=1}^r x_{ii}}{N} 100 \tag{1}$$

$$\text{Kappa Accuracy (KA)} = \frac{N \sum_{i=1}^r x_{ii} - \sum_{i=1}^r x_{i+} x_{+i}}{N - \sum_{i=1}^r x_{i+} x_{+i}} 100 \tag{2}$$

### 3. Results

#### 3.1. Development of Optimal Segmentation Parameters for Pleiades-1B and SPOT-6 images

The optimal parameters for Pleiades-1B and SPOT-6 images were determined by evaluating the overall and kappa accuracy results. The accuracies of all parameter combinations were compared. Tables 4–7 summarize the OA and KA of the selected combinations tested on the filtered and unfiltered images. This study shows that filtered images, both Pleiades-1B and SPOT 6 images, always produce better accuracy than unfiltered images. Unfiltered images (with a low-pass filter) tend to contain false (salt-and-pepper), which causes many misclassifications. In the Pleiades 1 B image, the best parameter combination was C6-MF from the filtered image in the combination [10]-[0.7]-[0.3] with a Kappa Accuracy (KA) of 83.2% and Overall Accuracy (OA) of 91% (Table 4), which is better than the best combination of unfiltered images on C7-UF, the combination [10]-[0.8]-[0.2] with a Kappa accuracy of 80.5% and an overall accuracy of 88.9% (Table 5). The same result was also found in the SPOT 6 image, which produced the best combination of the C7-MF combination [10]-[0.8]-[0.2] with OA 90.6% and KA 65.4% (Table 6), which is better than the SPOT 6 image unfiltered (Table 7) with OA 98.9% and KA 76.4%. This study also proves that the spatial resolution of the Pleiades with a spatial resolution of 0.5 m produces better accuracy than SPOT 6 imagery.

**Table 4.** The results of the combination of parameters using filtered Pleiades 1B image

Code	Combination of parameters*)	Accuracy measure (%)	
		KA	OA
C2-MF	[10]-[0.3]-[0.7]	82.0	89.8
C3-MF	[10]-[0.4]-[0.6]	81.0	90.2
C4-MF	[10]-[0.5]-[0.5]	82.4	90.3
C5-MF	[10]-[0.6]-[0.4]	73.0	87.0
C6-MF	[10]-[0.7]-[0.3]	83.2	91.0

Notes: \*) the combination of parameters [T]-[M]-[V] referred to in this table is a combination of tolerance values (the number on the far left), the mean (the number in the middle), and variance (the number on the far right)

**Table 5.** The results of the combination of parameters of unfiltered Pleiades 1B image

Code	Combination of parameters *)	Accuracy measure (%)	
		KA	OA
C1-UF	[10]-[0.2]-[0.8]	73.0	86.6
C3-UF	[10]-[0.4]-[0.6]	73.5	86.8
C4-UF	[10]-[0.5]-[0.5]	73.5	86.4
C5-UF	[10]-[0.6]-[0.4]	73.2	86.6
C7-UF	[10]-[0.8]-[0.2]	80.5	88.9

Notes: \*) the combination of parameters [T]-[M]-[V] referred to in this table is a combination of tolerance values (the number on the far left), the mean (the number in the middle), and variance (the number on the far right)

**Table 6.** The results of the combination of parameters of filtered Spot-6 image.

Code	Combination of parameters *)	Accuracy measure (%)	
		KA	OA
C1-MF	[10]-[0.2]-[0.8]	64.6	90.1
C2-MF	[10]-[0.3]-[0.7]	65.2	90.4
C3-MF	[10]-[0.4]-[0.6]	64.6	90.2
C4-MF	[10]-[0.5]-[0.5]	62.8	89.9
C6-MF	[10]-[0.7]-[0.3]	65.2	90.4
C7-MF	[10]-[0.8]-[0.2]	65.4	90.6

Notes: \*) the combination of parameters [T]-[M]-[V] referred to in this table is a combination of tolerance values (the number on the far left), the mean (the number in the middle), and variance (the number on the far right)

**Table 7.** The results are the combination of parameters unfiltered Spot-6 image

Code	Combination of parameters *)	Accuracy measure (%)	
		KA	OA
C3-UF	[10]-[0.4]-[0.6]	73.5	88.6
C4-UF	[10]-[0.5]-[0.5]	76.4	88.9
C7-UF	[10]-[0.8]-[0.2]	65.6	88.3

Notes: \*) the combination of parameters [T]-[M]-[V] referred to in this table is a combination of tolerance values (the number on the far left), the mean (the number in the middle), and variance (the number on the far right)

**3.2. Pleiades-1B Image Segmentation Using Filter (Lowpass) and Unfiltered**

The study examined various combinations of parameter values and found that low-pass-filtered Pleiades-1B image segmentation yielded the best five combinations of parameters. The combinations provided Kappa Accuracy (KA) values greater than 80%, namely C2-MF, C3-MF, C4-MF, and C6-MF (Figure 4). The study also found that the original Pleiades 1 B image (without a filter) obtained combinations with high accuracy, namely C1-UF, C3-UF, C4-UF, C5-UF, and C7-UF (Figure 4). The level of accuracy of OA and KA obtained on the Pleiades-1B image using a low-pass filter and without a filter was in the excellent category.

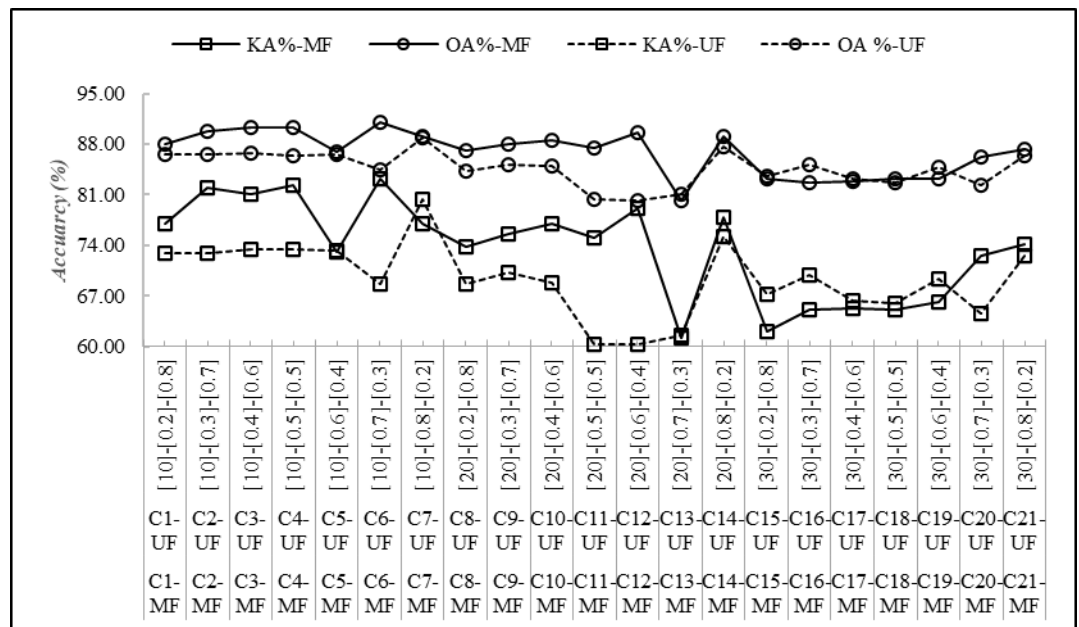


**Figure 4.** Combination of Pleiades 1b image parameters using filtering and unfiltering

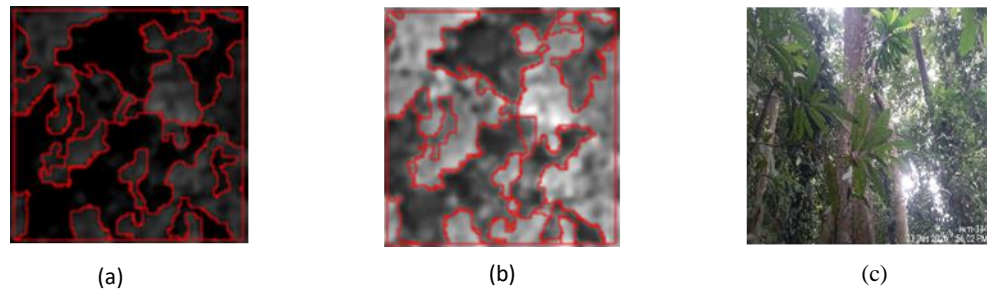


**Figure 5.** Combination of parameters of Pleiades-1B; (a) C6-MF image using filtering technique, (b) C7-UF image unfiltered, (c) sample field image

This study showed a difference in accuracy between segmentation using the original Pleiades-1B image and the filtered image. There were general differences in segmentation accuracy between segments using different tolerances (T). Tolerance (T) with a value of 10 is better than T values of 20 and 30, and the graph in Figure 4 shows that the accuracy at C1–C6 is relatively high. A lower accuracy at C7–C14 was found at a tolerance of 20. The study at C15–C21, with a tolerance of 30, provides a less accurate assessment. In general, the tolerance value tends to be small (T) 10, which provides better accuracy than the immense tolerance value (values 20 and 30). In this study, the tolerance value (T) 10 was the best measure of the value of the T parameter for distinguishing between the canopy and gap. In the unfiltered Pleiades-1B image, there is almost no change in accuracy, although there is a change in the T value from 0.4 to 0.6 (see Table 5). The segmentation accuracy is also strongly influenced by variations in the mean (M) and variance (V) values, as shown in Figure 5. The changes in M and V affect the accuracy (as shown in Figure 5). Mean value (M) with a value of 0.7 (filtered image with low pass/MF) and 0.8 in the unfiltered image (UF) gives the highest accuracy value. For the parameter value, the variance (V) is 0.3 for the MF image (filtered with low pass) and the variance (0.2) for the unfiltered (UF) image. The changes in the accuracy with different values of M and V are summarized in Tables 4 and 5.

### 3.3. Spot-6 Image Segmentation Using Filter (Lowpass) and Unfiltered

In contrast to the Pleiades-1B image, the filtered SPOT-6 image provided six optimal combinations with KA (Kappa Accuracy) of more than 61%, namely C1-MF, C2-MF, C3-MF, C4-MF, C6-MF, and C7-MF (Figure 6). The unfiltered SPOT-6 images received three combinations: C3-UF, C4-UF, and C7-UF.

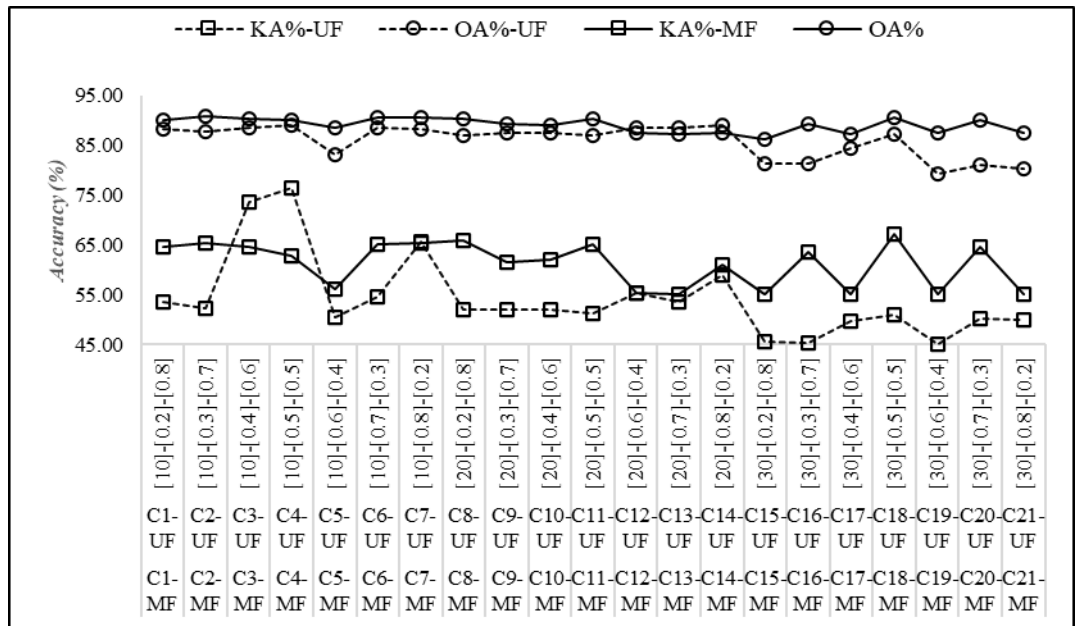


Figure 6. Combination of Pleiades 1b image parameters using filtering and unfiltering

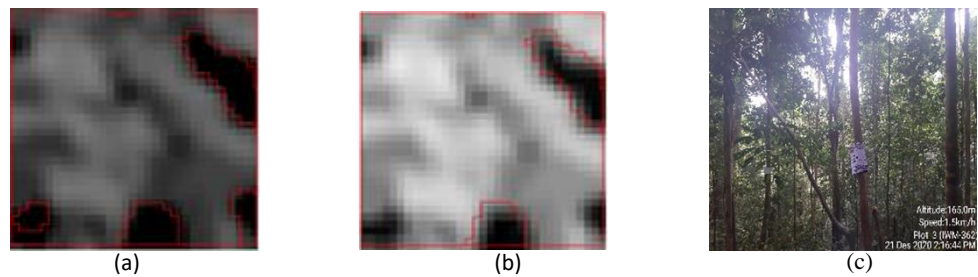


Figure 7 Combination of parameters of Spot-6; (a) C7-MF image using filtering technique, (b) C2-UF image unfiltered, (c) sample field foto

In this study, Spot-6, the tolerance parameter (T) value for the filtered and unfiltered Spot-6 images, showed a significant difference in accuracy (differences in OA and KA values). This study found that the best tolerance (T) parameter value in SPOT-6 image segmentation is the tolerance value (T),10 which gives a better level of accuracy than the tolerance value (20 and 30) (see Figure 6). Differences in accuracy also occurred in the mean (M) and variance (V) parameters. The Mean (M) values were 0.8-MF and 0.7-UF, while the variance (V) 0.2-MF and 0.3-UF values provided better accuracy in detecting crowns and gaps.

**3.4. Parameters of Segmentation on Filtered and Unfiltered Images of Pleides-1B**

From the data analysis, it was found that the low-pass-filtered Pleiades images consistently provided better accuracy than the infiltered images. This study found that noise from branch gaps (dark pixels) and bright pixels at the top canopy or branches should be eliminated. The study found that the low-pass filtered Pleiades-1B image provided the highest accuracy, with an overall accuracy of 91% and a kappa accuracy of 83.2%. Unfiltered images only provided overall accuracy of 88.1 % and a kappa accuracy of 80.15%. According to[19], a kappa accuracy index value of 40% was considered low, 40-80% was considered moderate, and 80% was very high. Using filtered images in the watershed segmentation algorithm can reduce over-segmentation. [20] the use of low-pass filters is very effectively applied to the watershed algorithm to segment broad-leaved and needle-leaved tree species with an accuracy of 80 to 90% using high-resolution imagery. Based on trial and error, the watershed algorithm's optimal similarity or scale parameter value was shown at a tolerance (T) value of 10. The object size resulting from the segmentation process is based on the value of the similarity parameter, which has been determined and defined. The larger the similarity value, the lower is the number of segments. The best mean and variance factor values for the filtered Pleiades-1B image are MF-[0.2], [0.3], [0.4], [0.5] [0.6], and [0.7], whereas for the

unfiltered Pleiades-1B image, the optimal mean and variance are UF-[0.2], [0.4], [0.5], [0.6], and [0.8]. The variance parameter is closely related to the data diversity. A variance value close to zero indicates that the data in each segment are increasingly homogeneous, with mean and variance parameter values of 0.5 for boreal forest ecosystems [5]. The greater the variance, the more significant the heterogeneity [12].

### 3.5. Segmentation Parameters on the Low-pass filtered and Unfiltered Spot-6 images.

The study showed that the segmentation of the filtered and unfiltered images provided different accuracy levels when identifying canopy and non-canopy cover. The low-pass filtered Spot-6 had an overall accuracy rate of 90.6% and kappa accuracy of 65.4%. The unfiltered Spot-6 image had an overall accuracy rate of 88.9% and a kappa accuracy rate of 76.4%. Based on a set of evaluated parameter combinations, this study found that the optimal tolerance parameter on the spot-6 image is the same as that on the Pleiades 1 B image, which is a scale of 10, while the mean and variance parameters are [0.3], [0.4], [0.5], and [0.7]. While the unfiltered Spot-6 image has a similarity tolerance value parameter of 10, the mean and variance factor values have only three optimal combinations, namely [0.3], [0.4], and [0.7]. The Pleiades-1B Image with a spatial resolution of 0.5 m provides better segmentation accuracy than the Spot-6 image with a 1.5 m spatial resolution. Thus, Iskandar et al. (2021), a very high spatial resolution image (Pleiades-1B Image) with a spatial resolution of 0.5 m provides better segmentation accuracy than a high spatial resolution image (Spot-6) with a 1.5 m spatial resolution, both on filtered and unfiltered images.

## 4. Conclusion

This study concluded that the best parameter combination of the watershed algorithm for detecting crown closure in Pleiades-1B is C6-MF [10]-[0.7]-[0.3], with an overall accuracy level of 91.0% and a Kappa accuracy of 83.2%. In the Spot-6 imagery, the best parameter combination was C7-MF[10]-[0.8]-[0.2], with a 90.6% overall accuracy rate and 65.4% kappa accuracy. The study also concluded that low-pass filtered images provided better accuracy than unfiltered images for both Pleiades-1B and SPOT-6 images. The very high spatial resolution Pleiades-1B Image of 0.5 m provided better segmentation accuracy than the high-spatial-resolution image (SPOT-6 Image) with a 1.5 m spatial resolution.

## Conflicts of interest

There are no conflicts to declare

## References

- [1] Blaschke, T. Object Based Image Analysis for Remote Sensing. *ISPRS J. Photogramm. Remote Sens.* **2010**, *65*, 2–16, doi:10.1016/j.isprsjprs.2009.06.004.
- [2] Blaschke, T.; Hay, G.J.; Kelly, M.; Lang, S.; Hofmann, P.; Addink, E.; Queiroz Feitosa, R.; van der Meer, F.; van der Werff, H.; van Coillie, F.; et al. Geographic Object-Based Image Analysis - Towards a New Paradigm. *ISPRS J. Photogramm. Remote Sens.* **2014**, *87*, 180–191, doi:10.1016/j.isprsjprs.2013.09.014;
- [3] Tarabalka, Y.; Chanussot, J.; Benediktsson, J.A.; Angulo, J.; Fauvel, M. Segmentation and Classification of Hyperspectral Data Using Watershed. *Int. Geosci. Remote Sens. Symp.* **2008**, *3*, 652–655, doi:10.1109/IGARSS.2008.4779432.
- [4] Chen, S.; Luo, J.; Shen, Z.; Hu, X.; Gao, L. Segmentation of Multi-Spectral Satellite Images Based on Watershed Algorithm. *Proc. - 2008 Int. Symp. Knowl. Acquis. Model. KAM 2008* **2008**, 684–688, doi:10.1109/KAM.2008.84.
- [5] Räsänen, A.; Rusanen, A.; Kuitunen, M.; Lensu, A. What Makes Segmentation Good? A Case Study in Boreal Forest Habitat Mapping. *Int. J. Remote Sens.* **2013**, *34*, 8603–8627, doi:10.1080/01431161.2013.845318.

- [6] Paul, S.S.; Li, J.; Wheate, R.; Li, Y. Application of Object Oriented Image Classification and Markov Chain Modeling for Land Use and Land Cover Change Analysis. *J. Environ. Informatics* **2018**, *31*, 30–40, doi:10.3808/jei.201700368.
- [7] Wang, L.; Gong, P.; Ying, Q.; Yang, Z.; Cheng, X.; Ran, Q. Settlement Extraction in the North China Plain Using Landsat and Beijing-1 Multispectral Data with an Improved Watershed Segmentation Algorithm. *Int. J. Remote Sens.* **2010**, *31*, 1411–1426, doi:10.1080/01431160903475332.
- [8] Hong, Y.; Chiang, Y.M.; Liu, Y.; Hsu, K.L.; Sorooshian, S. Satellite-Based Precipitation Estimation Using Watershed Segmentation and Growing Hierarchical Self-Organizing Map. *Int. J. Remote Sens.* **2006**, *27*, 5165–5184, doi:10.1080/01431160600763428.
- [9] Zhang, W.; Jiang, D. The Marker-Based Watershed Segmentation Algorithm of Ore Image. *2011 IEEE 3rd Int. Conf. Commun. Softw. Networks, ICCSN 2011* **2011**, 472–474, doi:10.1109/ICCSN.2011.6014611.
- [10] Jiang, K.; Liao, Q.M.; Dai, S.Y. A Novel White Blood Cell Segmentation Scheme Using Scale-Space Filtering and Watershed Clustering. *Int. Conf. Mach. Learn. Cybern.* **2003**, *5*, 2820–2825, doi:10.1109/icmlc.2003.1260033.
- [11] Gupta, V.; Gandhi, D.K.; Yadav, P. Removal of Fixed Value Impulse Noise Using Improved Mean Filter for Image Enhancement. *2013 Nirma Univ. Int. Conf. Eng. NUiCONE 2013* **2013**, 1–5, doi:10.1109/NUiCONE.2013.6780117.
- [12] Hossain, M.D.; Chen, D. Segmentation for Object-Based Image Analysis (OBIA): A Review of Algorithms and Challenges from Remote Sensing Perspective. *ISPRS J. Photogramm. Remote Sens.* **2019**, *150*, 115–134, doi:10.1016/j.isprs.2019.02.009.
- [13] Vincent, L.; Soille, P. Watersheds in Digital Spaces: An Efficient Algorithm Based on Immersion Simulations. *IEEE Trans. Pattern Anal. Mach. Intell.* **1991**, *13*, 583–598, doi:10.1109/34.87344.
- [14] Jyothish, V.R.; Bindu, V.R.; Greeshma, M.S. An Efficient Image Segmentation Approach Using Superpixels with Colorization. *Procedia Comput. Sci.* **2020**, *171*, 837–846, doi:10.1016/j.procs.2020.04.091.
- [15] Tang, Y.; Zhao, L.; Ren, L. Different Versions of Entropy Rate Superpixel Segmentation for Hyperspectral Image. *2019 IEEE 4th Int. Conf. Signal Image Process. ICSIP 2019* **2019**, 1050–1054, doi:10.1109/SIPROCESS.2019.8868344.
- [16] Hoiem, D.; Efros, A.A.; Hebert, M. Recovering Surface Layout from an Image. *Int. J. Comput. Vis.* **2007**, *75*, 151–172, doi:10.1007/s11263-006-0031-y.
- [17] FUSING INFORMATION FROM SUBPIXEL TO SUPERPIXEL FOR HYPERSPECTRAL ANOMALY DETECTION Zhihong Huang, Shutao Li, and Leyuan Fang College of Electrical and Information Engineering, Hunan University, Changsha, China, 410082. **2018**, 1260–1263.
- [18] Liu, Y.; Cao, G.; Sun, Q.; Siegel, M. Hyperspectral Classification via Deep Networks and Superpixel Segmentation. *Int. J. Remote Sens.* **2015**, *36*, 3459–3482, doi:10.1080/01431161.2015.1055607.
- [19] Landis, J.R.; Koch, G.G. Landis and Koch 1977\_agreement of Categorical Data. *Biometrics* **1977**, *33*, 159–174.
- [20] Kanda, F.; Kubo, M.; Muramoto, K. Watershed Segmentation and Classification of Tree Species Using High Resolution Forest Imagery. *Int. Geosci. Remote Sens. Symp.* **2004**, *6*, 3822–3825, doi:10.1109/igarss.2004.1369956.